VISUAL SIMULATION OF MAGNETIC FLUIDS

Tomokazu Ishikawa[1], Yonghao Yue[1], Kei Iwasaki[2], Yoshinori Dobashi[3] and Tomoyuki Nishita[1]
[1]*The University of Tokyo, Tokyo, Japan*
[2]*Wakayama University, Wakayama, Japan*
[3]*Hokkaido University, Sapporo, Japan*

Keywords: Magnetic Fluids, SPH (Smoothed Particle Hydrodynamics) Method, Magnet Simulation, Spiking Phenomenon.

Abstract: In this paper, we focus on simulation of magnetic fluids. Magnetic fluids behave as both fluids and as magnetic bodies, and these characteristics allow them to generate 'spike-like' shapes along a magnetic field. Magnetic fluids are popular materials for use in works of art. Our goal is to simulate such works of art. In the field of electromagnetic hydrodynamics, many methods have also been proposed for simulating such spike shapes based on numerical fluid analysis. However, those methods are computationally expensive and they typically require tens of hours just to simulate a single spike. We propose a more efficient method by combining a procedural approach and the SPH method (smoothed particle hydrodynamics). Our method simulates overall behaviors of the magnetic fluids using the SPH method and then synthesizes the spike shapes by using the procedural approach. We demonstrate our method can generate visually plausible results within a reasonable computational cost.

1 INTRODUCTION

In the field of computer graphics, fluid simulation is one of the most important research topics. Many methods have therefore been proposed to simulate realistic motion of fluids by introducing physical laws. Previous methods have attempted to simulate incompressible fluids, such as smoke, water and flames, as well as compressible fluids such as explosions and viscous fluids (Stam, 1999) (Fedkiw et al., 2001) (Goktekin et al., 2004) (Yngve et al., 2000). In this paper, we focus on visual simulation of magnetic fluids.

A magnetic fluid is a colloidal solution consisting of micro-particles of ferromagnetic bodies, a surfactant that covers the magnetic micro-particles, and a solvent that acts as the base (see Fig.1). Therefore, magnetic fluids behave as both fluids and as magnetic bodies and can be magnetized and attracted to a magnet. Thanks to the controllability of the shapes of the magnetic fluids by magnetic forces, magnetic fluids have been widely used for various products such as electrical and medical equipments. A more interesting application of the magnetic fluids have appeared for creating new works of art. When a magnet is located near a magnetic fluid, the magnetic fluid forms spiky shapes like horns along the direction of the magnetic field generated by the magnet (see Fig. 2). This is known as the 'spiking phenomenon'. The art work using the magnetic fluids utilizes this phenomenon and generates interesting shapes by applying magnetic forces to the fluids.

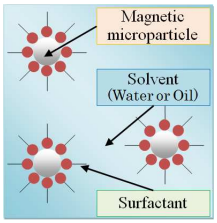

Figure 1: Structure material of magnetic fluid.

Magnetic fluids have been studied extensively in the field of electromagnetic hydrodynamics. The phenomena covered by electromagnetic hydrodynamics can be further classified into plasma and magnetic fluids. A plasma is an electromagnetic fluid that generally has charge (i.e. an electric current flows) but does not have any defined interfaces (or free surfaces). The dynamics of aurora, prominence, and flares in the

Ishikawa T., Yue Y., Iwasaki K., Dobashi Y. and Nishita T..
VISUAL SIMULATION OF MAGNETIC FLUIDS.
DOI: 10.5220/0003867303190327
In *Proceedings of the International Conference on Computer Graphics Theory and Applications* (GRAPP-2012), pages 319-327
ISBN: 978-989-8565-02-0

Figure 2: Spiking phenomenon of magnetic fluid (photograph).

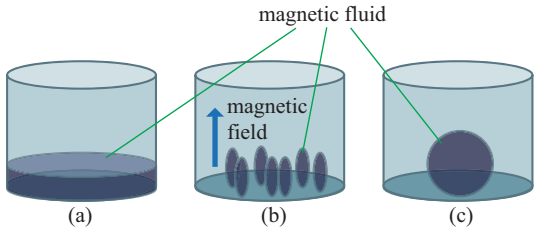

Figure 3: Potentiality of shapes of magnetic fluid. (a), (b) and (c) show the state with minimum potential energy, minimum magnetic energy and minimum surface energy, respectively.

sun can be calculated by simulating a plasma. On the other hand, a magnetic fluid has usually interfaces but does not have any charges. We can find a few researches on the visual simulation of these phenomena in the field of computer graphics. However, to the best of our knowledge, no methods have been proposed for simulating the magnetic fluids in the field of computer graphics. Although we could use techniques developed in the field of magnetohydrodynamics, their computational cost is extremely high (Yoshikawa et al., 2011). They typically require tens of hours to simulate a single spike only.

We therefore propose an efficient and visually plausible method for simulating the spiking phenomenon, aiming at the virtual reproduction of the art work. Our method combines a procedural approach and the SPH (smoothed particle hydrodynamics) method. The SPH method is used to compute overall surfaces of the fluid with a relatively small number of particles. Then, we generate the spike shapes procedurally onto the fluid surface. Although our method is not fully physically-based, it is easy to implement and we can reproduce spike shapes that are similar to those observed in the real magnetic fluids.

2 RELATED WORK

Many methods have been proposed to simulate incompressible fluids such as smoke and flames (Stam, 1999) (Fedkiw et al., 2001). Goktekin et al. proposed a simulation method for viscoelastic fluids by incorporating an elastic term into the Navier Stokes equations (Goktekin et al., 2004).

Stam and Fuime introduced the SPH method into the CG field for representing flames and smoke (Stam and Fiume, 1995). Müller et al. proposed a SPH-based method based to simulate fluids with free surfaces (Müller et al., 2003). Recently, many methods using the SPH method have been proposed, e.g., simulation of viscoelastic fluids (Clavet et al., 2005), interaction of sand and water (Rungjiratananon et al., 2008), and fast simulation of ice melting (Iwasaki et al., 2010). Our method also uses the SPH method and to simulate the magnetic fluids.

In computer graphics, no methods have been proposed for simulating electromagnetic hydrodynamics. Although a technique for simulating the magnetic field was proposed by Thomaszewski et al (Thomaszewski et al., 2008), only the magnetism of rigid bodies is calculated as an influence of magnetic fields. Baranoski proposed a visual simulation method for the aurora by means of simulating the interaction between electrons and the magnetic field using particles with an electrical charge (Baranoski et al., 2003) (Baranoski et al., 2005). However, these methods do not take into account fluid dynamics.

In the field of physics, the characteristics of magnetic fluids have been studied since 1960. Rosenswig demonstrated spiking phenomena by using quantitative analysis (Rosensweig, 1987). Sudo et al. have studied the effects of instability, not only in the spiking phenomenon, but also on the surfaces of magnetic fluids (Sudo et al., 1987). Han et al. modeled the formation of a chain-shape between colloidal particles according to the magnetization of the particles(Han et al., 2010). Combined with a lattice Boltzmann method, they showed that the colloidal particles would form lines along the magnetic field. However, their method cannot represent the spike shapes. Yoshikawa et al. combined the MPS (Moving particle Semi-implicit) method with the FEM (Finite Element Method) and simulated magnetic fluids. Even when using 100,000 particles and a mesh with 250,000 tetrahedra, they were able to reproduce only a single spike (Yoshikawa et al., 2011).

3 SPIKING PHENOMENON

Before explaining our simulation approach, we will describe the mechanism about the formation of the spike shape (Rosensweig, 1987). There are three important potential energies E_g, E_{mag} and E_s that relate

to the formation mechanism.

E_g is the potential energy of gravity. If only the gravity is applied as an external force to the magnetic fluid, the fluid will form a horizontal surface at a constant height, as shown in Fig. 3 (a), since E_g is at the minimum level under this condition. E_{mag} is the magnetic potential energy. If only the magnetic force is applied as an external force, the fluid will form a certain number of spheroids that stand at the bottom of the vessel, as shown in Fig. 3 (b). E_{mag} is at a minimum level under these conditions. E_s is the surface energy. If the surface tension alone is applied as the external force, the fluid will form into a spherical shape, as shown in Fig. 3 (c). E_s is at the minimum level under these conditions. The actual shape is the one that minimizes the summation of these three energies, resulting in spike-like shapes, as shown in Fig. 2.

Therefore, in order to simulate the spiking phenomena, the three forces need to be taken into account: the gravity, magnetic forces, and the surface tension. At the early stages of this research, we tried to simulate the spiking phenomenon by using the SPH method only. However, it turned out that we could not reproduce the spikes unless we used a significant number of particles, resulting in a very long computation time. Thus, we use the SPH method to simulate the overall behavior of the fluids and develop a new procedural method to generate the spike shapes. Details of our method is described in the following sections.

4 OUR SIMULATION METHOD

As we described before, our method combines the SPH method and a procedural approach. In this section, we first describe the governing equations of the magnetic fluid that are solved by using the SPH method (Section 4.1). Next, we describe the computation of the magnetic force applied to each particle and a technique for generating the fluid surface by using the result of the SPH simulation (Section 4.2). Then, we describe the procedural method for computing the spike shape (Section 4.3).

4.1 Governing Equations

The behavior of incompressible fluids is described by the following equations.

$$\nabla \cdot \mathbf{u} = 0, \quad (1)$$

$$\frac{\partial \mathbf{u}}{\partial t} = -(\mathbf{u} \cdot \nabla)\mathbf{u} - \frac{1}{\rho}\nabla p + \nu \nabla^2 \mathbf{u} + \mathbf{F}. \quad (2)$$

Equation (1) is the continuity equation, and Navier-Stokes equation (Equation (2)) describes the conservation of momentum. $\mathbf{u}$ is the velocity vector, t is time, ρ is the fluid density, p is the pressure and ν is the kinematic viscosity coefficient. $\mathbf{F}$ is the external force that includes the gravity, the magnetic force, and the surface tension (Iwasaki et al., 2010).

Our method solves the above equations by using the SPH method. That is, the magnetic fluids are represented by a set of particles and the motion of the fluids is simulated by calculating the motions of the particles. For this calculation, we use the method developed by Iwasaki et al (Iwasaki et al., 2010). This method is significantly accelerated by using the GPU and is capable of simulating water. We extend the method to the simulation of magnetic fluids. The difference of magnetic fluids from the non-magnetic fluids is that the magnetic force is induced when magnetic field exists. The computation of the magnetic force is described in the next subsection.

4.2 Calculation of Magnetization and Magnetic Force

Each particle represents a small magnetic fluid element, and its motion is calculated by taking into account the properties of both fluid and magnetic body. To calculate the magnetic force, our method assumes the paramagnetism, that is, each particle does not have any magnetic charges if there is no external magnetic field. However, if a magnetic field is applied, each particle becomes magnetized in the direction along the applied magnetic field. In this paper, we assume that the magnetic field is induced by a bar magnet placed near the fluid. In order to handle a magnet with an arbitrary shape, we can use the method developed by Thomaszewski et al (Thomaszewski et al., 2008).

The magnetic field is calculated by approximating the bar magnet as a magnetic dipole. We assume that the north and south poles of the magnetic bar have an equal magnitude of magnetic charge but the signs are different (positive or negative). When computing the magnetic force working on each particle, it is not sufficient to calculate only the force induced directly by the magnetic bar. This is due to the paramagnetism. When each particle is placed in the magnetic field of the magnetic bar, the particle is magnetized and works as if it were a small spherical magnet. Therefore, our method first computes the magnetic field at equilibrium state, taking into account the magnetization of the particles. After that, the magnetic force for each particle is calculated. The details are described in the following.

The magnetic moment $\mathbf{m}$ due to a magnetic dipole

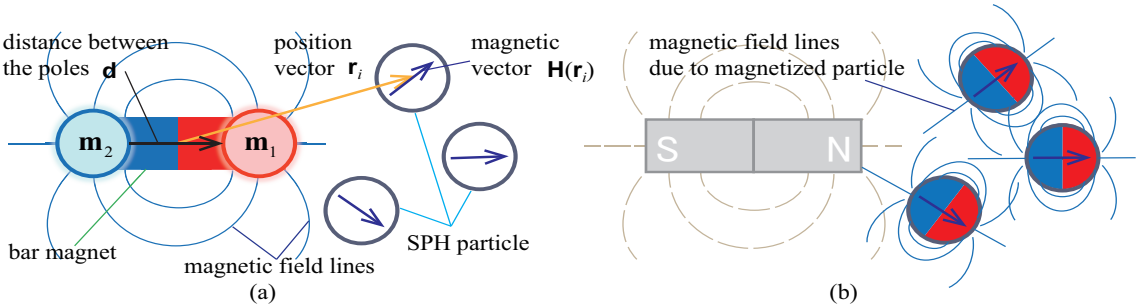

Figure 4: Calculation of the magnetization and the magnetic force. (a) First, we calculate the magnetic field vector at each SPH particle induced by a magnetic dipole. (b) Next, we calculate the influence of other particles from the magnetized particles.

Figure 5: Photograph of a real magnetic fluid surface.

Figure 6: The surface computed using Equation (13).

is defined by the following equation:

$$\mathbf{m} = q_m \mathbf{d}, \tag{3}$$

where q_m is the magnitude of the magnetic charge and $\mathbf{d}$ is a vector connecting from the south to north poles. We call the magnetic vector induced by the magnetic bar as a background magnetic vector. Let us assume that the origin is at the midpoint between the north and the south poles. Then, the background magnetic vector $\mathbf{H}_{dipole}(\mathbf{r})$ at position $\mathbf{r}$ is expressed by the following equation.

$$\mathbf{H}_{dipole}(\mathbf{r}) = -\frac{1}{4\pi\mu}\nabla\frac{\mathbf{m}\cdot\mathbf{r}}{r^3}, \tag{4}$$

where μ is the permeability of the magnetic fluid and $r = |\mathbf{r}|$. Each particle is magnetized due to the background magnetic vector field and induces an additional magnetic vector field. Thus, in order to obtain the final magnetic vector $\mathbf{H}(\mathbf{r}_j)$ at particle j, the magnetic interactions between particles have to be computed by solving the following equation,

$$\mathbf{H}(\mathbf{r}_j) = \mathbf{H}_{dipole}(\mathbf{r}_j) - \frac{V}{4\pi\mu}\sum_{\substack{i=1\\ i\neq j}}^{N}\nabla\frac{\chi\mathbf{H}(\mathbf{r}_i)\cdot\mathbf{r}_{ij}}{r_{ij}^3}, \tag{5}$$

where V is the volume of a particle and we assume that the volume of all particles are equal, $\mathbf{r}_i$ is the position of particle i, N is the total number of particles, χ is the magnetic susceptibility. $\mathbf{r}_{ij} = \mathbf{r}_j - \mathbf{r}_i$, and $r_{ij} = |\mathbf{r}_j - \mathbf{r}_i|$. The magnetic susceptibility changes due to the external magnetic field. It is known that the magnetization of the magnetic fluids is saturated when the magnitude of an external magnetic field is larger. We calculate the magnetization in all particles based on the actual relationship between the magnetization and an external magnetic field in (Yoshikawa et al., 2011). The gradient part of the second term in Equation (5) is calculated by the following equation,

$$\nabla\frac{\chi\mathbf{H}(\mathbf{r}_i)\cdot\mathbf{r}_{ij}}{r_{ij}^3} = \nabla(\chi\mathbf{H}(\mathbf{r}_i))\cdot\frac{\mathbf{r}_{ij}}{r_{ij}^3} + \chi\mathbf{H}(\mathbf{r}_i)\cdot\nabla(\frac{\mathbf{r}_{ij}}{r_{ij}^3}). \tag{6}$$

We use the kernel function to calculate the partial differential of $\mathbf{H}(\mathbf{r}_i)$, that is,

$$\nabla(\chi\mathbf{H}(\mathbf{r}_i)) = \sum_{\substack{j=1\\ j\neq i}}^{N}\frac{m_j}{\rho_j}\chi\mathbf{H}(\mathbf{r}_j)\nabla w(r_{ij}), \tag{7}$$

where $w(r_{ij})$ is the kernel function. We use the following kernel function frequently refered in the SPH method (Müller et al., 2003),

$$w(r) = \begin{cases} \frac{315}{64\pi h^9}(h^2 - r^2)^3 & 0 \le r \le h \\ 0 & h < r, \end{cases} \tag{8}$$

where h is the effective radius of each particle. We calculate Equation (5) taking into account the influences from all the particles. We use the Gauss-Seidel method to solve Equation (5).

Next, the magnetic force $\mathbf{F}_{mag}(\mathbf{r}_i)$ is calculated by using the following equation (Rosensweig, 1987),

$$\mathbf{F}_{mag}(\mathbf{r}_i) = -\nabla\phi_i(\mathbf{r}_i), \tag{9}$$

where,

$$\phi_i = \frac{\mu \mid \mathbf{H}(\mathbf{r}_i) \mid^2}{2}. \tag{10}$$

$\nabla\phi_i$ in Equation (9) is calculated by using the kernel function represented by Equation (8), that is,

$$\nabla\phi_i = \sum_j m_j \frac{\phi_j}{\rho_j} \nabla w(r_{ij}). \tag{11}$$

4.3 Computing Spike Shapes

The formation of the small spike shapes on the magnetic fluid surface can be explained by the balance among the forces of the surface tension, gravity and the stress due to magnetization (Rosensweig, 1987)DAs we described before, our method synthesizes the spike shapes by employing the procedural approach. The basic idea is as follows. We prepare a procedural height field representing the spike shapes generated on a flat surface. Next, during the simulation, the height field is mapped onto the curved surface calculated by using the SPH particles. When the fluid surface is flat and a magnetic field is perpendicular to the flat surface, the spike shapes can be represented as a height field $z(x, y)$ expressed by the following equation (see 7 for derivation).

$$z(x,y) = \sum C_0(\sin k_1 x + C_1 \cos k_1 x)(\sin k_2 y + C_2 \cos k_2 y), \tag{12}$$

where C_i (i = 0, 1, 2), k_1 and k_2 are parameters controlling the spike shapes. There is a constraint on k_1 and k_2: these need to be integers that satisfy $k_1^2 + k_2^2$ is the same for possible combinations of k_1^2 and k_2^2. Σ means the sum of the possible combinations. For the real magnetic fluids, a regular hexagonal pattern is often observed (see Fig. 5). Therefore, we choose the constants in Equation (12) so that such a pattern can be reproduced:

$$z(x,y) = C_0(\cos\frac{k}{2}(\sqrt{3}x+y) + \cos\frac{k}{2}(\sqrt{3}x-y) + \cos ky). \tag{13}$$

The above equation is used for the procedural height field representing the spike shapes on a flat surface. We set k to 50. Fig. 6 shows an example of the spike shapes synthesized by using Equation (13). Compared to Fig. 5, we can see that the synthesized shape is very similar to the real spike shapes. The size of the spike is controlled by adjusting C_0. We simply assume that C_0 is proportional to the magnitude of the magnetic field.

$$C_0 = \beta \mid \mathbf{H}(\mathbf{x}) \mid, \tag{14}$$

where, β is the proportional coefficient, $\mid \mathbf{H}(\mathbf{x}) \mid$ is the magnitude of the magnetic field at position $\mathbf{x}$.

In the real world, the following three structural features are observed: 1) positions of the spikes are symmetric as shown in Fig. 5, 2) distances between neighboring spikes become shorter when the magnetic force becomes stronger, and 3) the spikes are formed along the direction of the magnetic field lines. We develop a mapping method so that these three features are reproduced.

First, we set the intersection between the extended line connecting a magnetic dipole and the fluid surface to the origin of the texture coordinate defined by xy in Equation (13). This is because the magnetic field created from one magnet becomes symmetrical field with respect to a point centering on magnet. We trace six directions from the origin of the texture coordinates and calculate the mapping coordinates of the vertices of the spike because the height field reproduced by Equation (13) has three axes of symmetry (see Fig. 7 (a)). Let $\mathbf{x}_0$ be the position of the top of the spike just above the magnet. For each direction of six tangent vectors align to the three axes, the position of n-th spike $\mathbf{x}_n$ from the origin is calculated by the following equation,

$$\mathbf{x}_n = \mathbf{x}_{n-1} + l(\mathbf{H}(\mathbf{x}_0))\mathbf{d}_{n-1}, \tag{15}$$

where l is a function representing the distance between the tops of $n-1$-th and n-th spikes and it is determined by $\mathbf{H}(\mathbf{x}_0)$. $\mathbf{d}_{n-1}$ is the tangent vector on the fluid surface at the mapping coordinate $\mathbf{s}_{n-1}$. Experimentally, we used $l = \frac{\alpha}{|\mathbf{H}(\mathbf{x}_0)|}$, where α = 0.15.

To represent the characteristics that the spikes grow along the direction of the magnetic field lines, we calculate the magnetic field vector at $\mathbf{x}_1$, and we calculate the intersection between the fluid surface and the magnetic field vector. The intersection point is the mapping coordinate $\mathbf{s}_1$. By repeatedly applying this operation to a mapping area, we calculate the mapping coordinates.

The positions of the tops of the spikes between two adjacent symmetry axes (red points in Fig. 7 (c)) are calculated by interpolating the positions of two n-th spikes (yellow points in Fig. 7 (c)).

The mapping area is determined by using the particles whose magnitudes of the magnetizations are greater than a threshold. The magnitude of magnetization is calculated by the balanced equation (Equation (26)) for simple spike shapes in equilibrium (see 7). We use the minimum value of the magnetization M_c as the threshold. M_c is calculated by the following equation,

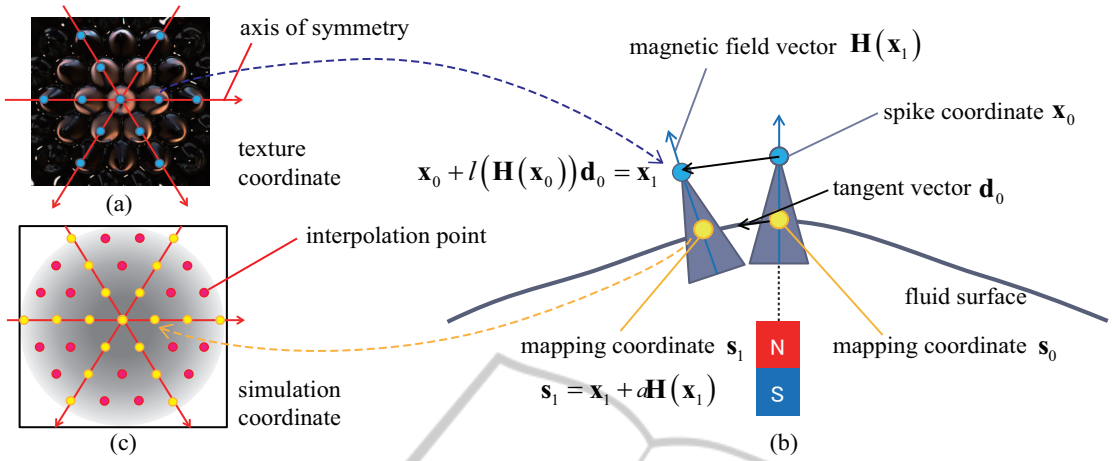

Figure 7: (a) Spike texture coordinates are used as the height field. (b) To calculate the coordinates of the spike vertices, we trace along the fluid surface. (c) The coordinates other than an axis of symmetry are calculated by interpolation.

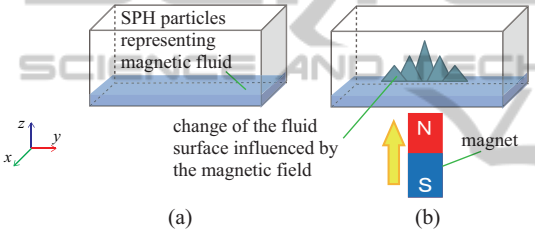

Figure 8: The simulation space of our method. (a) The magnetic fluids, which are represented by a set of SPH particles, are stored in a cubic container. (b) The magnet is located underneath the container. Then the motions of the magnet fluids are simulated by moving the magnet.

$$M_c^2 = \frac{2}{\mu}(1+\frac{1}{\gamma})\sqrt{(\rho_1-\rho_2)g\kappa}, \qquad (16)$$

where ρ_1 and ρ_2 are the density of the magnetic fluid and air, respectively. κ is the magnitude of the surface tension.

5 RENDERING

The surfaces of the magnetic fluids are extracted by using the method proposed by Yu et al. (Yu and Turk, 2010). Since the magnetic fluids are colloid fluids, the transmitted light in the magnetic fluids is scattered. However, since the colors of the magnetic fluids are black or brown in general, the albedo of magnetic fluids is very small. Thus, the light scattering effects inside the magnetic fluids are negligible. Therefore, our method ignores the light scattering inside the magnetic fluids. We used POV-Ray to render the surfaces.

6 RESULTS

For the simulation of our method, we used CUDA for the SPH method and the calculation of the magnetic force at each SPH particle. The number of particles used in the simulation shown in Figs. 9 and 10 is 40,960. The average computation time of the simulation for a single time-step is 6 milliseconds on a PC with an Intel(R) Core(TM)2 Duo 3.33GHz CPU, 3.25GB RAM and an NVIDIA GeForce GTX 480 GPU. The parameters used in the simulation are shown in Table 1. The average computation time of the surface construction for a frame is 2 minutes on the same PC. The initial fluid surface is shown in Fig. 8 (a). The fluid is contained in a box, which is not shown. Fig. 8 (b) shows how the shape of the fluid surface changes when a magnet approaches the bottom of the box. Fig. 9 shows an animation sequence of the magnetic fluid when we move the magnet in the vertical direction. As shown in Fig. 9, the spikes grow and increase when the magnet moves closer to the magnetic fluids. Fig. 10 shows an animation sequence of the magnetic fluid when we eliminate the magnet field. The surface becomes flat as we decrease the magnitude of the magnetic field. These results demonstrate that our method can simulate the paramagnetic property of magnetic fluids. Fig.9 shows an animation of magnetic fluids with the movement of a magnet. As shown in Fig.9, the spikes grow and increase when we move the magnet closer to the magnetic fluids. These results demonstrate that our method can simulate the paramagnetic property of magnetic fluids. Fig. 11 shows an example where we use two magnets. Compared to the case when using only a single magnet, the directions of the spikes get

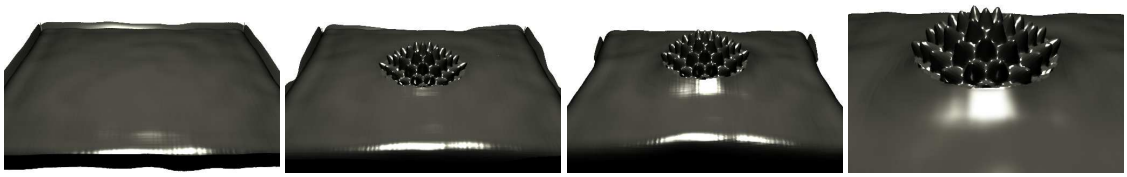

(a) t = 1.6 sec. (b) t = 3.2 sec. (c) t = 4.8 sec. (d) Enlarged view of (c).

Figure 9: Formation of spikes in the magnetic fluids. Spike shapes grow as the magnet approaches the bottom of the magnetic fluids.

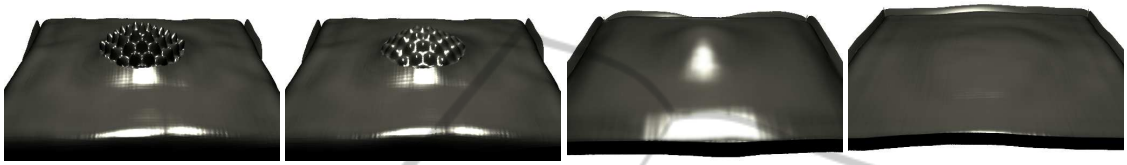

(a) t = 5.2 sec. (b) t = 6.8 sec. (c) t = 8.4 sec. (d) t = 10.0 sec.

Figure 10: Magnet fluids act as fluids when the magnetic field is reduced.

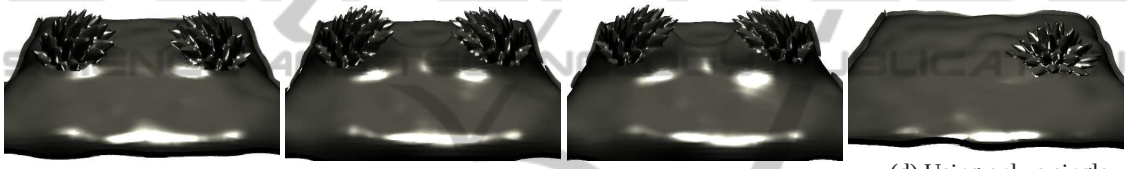

(a) t = 5.2 sec. (b) t = 6.8 sec. (c) t = 8.4 sec. (d) Using only a single magnet.

Figure 11: (a) to (c) show the results of the magnet fluids and the spikes by setting two magnets under the magnetic fluids. (d) shows the simulation result of the spikes using a single magnet for comparison. Compared with (d), the spikes closer to the other magnet get mush distorted in (a) to (c), the spikes which are closer to the other magnet get much distorted.

Table 1: Parameter setting of magnetic fluid simulation.

param.	meaning	value
dt	time step	0.00075
ν	kinematic viscosity coefficient	0.12
m	particle mass	0.016
R	particle radius	0.5
h	effective radius	1.3
g	gravitational acceleration	9.8
k	coefficient of surface tension	7.5
q_m	magnitude of the magnetic charge	5.0
μ	permeability of the magnetic fluid	$4\,\pi \times 10^{-7}$
χ	magnetic susceptibility	0.01

changed according to the change in the magnetic field due to the other magnet.

7 CONCLUSIONS AND FUTURE WORK

We have proposed a visual simulation method for magnetic fluids whose shapes change according to the magnetic field. We compute the spike shapes using a procedural approach, and map the shapes onto the fluid surface. Our method demonstrates that the magnitude of the magnet field influences the shapes of the magnet fluids and the magnet fluids act as fluids when the magnet field is eliminated. There are three limitations for our method. First, the conservation of the fluid volume is not considered when mapping the spike shapes onto the fluid surface. Second, our method cannot handle the fusion of more than one spike shapes, while we can observe such a fusion in real magnetic fluids. Third, our method does not simulate the flows of spikes along the velocity and vorticity of the magnetic fluid, since the function used for representing the spike shapes is not changed by the fluid behavior.

In future work, we would like to calculate the spike pattern other than regular hexagonal pattern dynamically using Equation (12) and represent the other spike shape arrangement. Moreover, to apply our method to works of art, we would like to control the magnetic field by using electric current flows.

REFERENCES

Baranoski, G., Rokne, J., Shirley, P., Trondsen, T., and Bastos, R. (2003). Simulation the aurora. *Visualization and Computer Animation*, 14(1):43–59.

Baranoski, G., Wan, J., Rokne, J., and Bell, I. (2005). Simulating the dynamics of auroral phenomena. *ACM Transactions on Graphics (TOG)*, 24(1):37–59.

Clavet, S., Beaudoin, P., and Poulin, P. (2005). Particle-based viscoelastic fluid simulation. In *Proceedings of the 2005 ACM SIGGRAPH/Eurographics symposium on Computer animation*, pages 219–228. ACM, ACM.

Cowley, M. D. and Rosensweig, R. E. (1967). The interfacial stability of a ferromagnetic fluid. *Journal of Fluid Mechanics*, 30(4):671–688.

Fedkiw, R., Stam, J., and Jensen, H. W. (2001). Visual simulation of smoke. In *Proceedings of SIGGRAPH 2001*, Computer Graphics Proceedings, Annual Conference Series, pages 15–22. ACM, ACM Press / ACM SIGGRAPH.

Goktekin, T. G., Bargteil, A. W., and OfBrien, J. F. (2004). A method for animating viscoelastic fluids. In *Proceedings of SIGGRAPH 2004*, Computer Graphics Proceedings, Annual Conference Series, pages 463–468. ACM, ACM Press / ACM SIGGRAPH.

Han, K., Feng, Y. T., and Owen, D. R. J. (2010). Three-dimensional modelling and simulation of magnetorheological fluids. *International Journal for Numerical Methods in Engineering*, 84(11):1273–1302.

Iwasaki, K., Uchida, H., Dobashi, Y., and Nishita, T. (2010). Fast particle-based visual simulation of ice melting. *Computer Graphics Forum (Pacific Graphics 2010)*, 29(7):2215–2223.

Müller, M., Charypar, D., and Gross, M. (2003). Particle-based fluid simulation for interactive applications. In *Proceedings of the 2003 ACM SIGGRAPH/Eurographics symposium on Computer animation*, pages 154–159. ACM, ACM.

Rosensweig, R. (1987). Magnetic fluids. *Annual Review of Fluid Mechanics*, 19:437–461.

Rungjiratananon, W., Szego, Z., Kanamori, Y., and Nishita, T. (2008). Real-time animation of sand-water interaction. *Computer Graphics Forum (Pacific Graphics 2008)*, 27(7):1887–1893.

Stam, J. (1999). Stable fluids. In *Proceedings of SIGGRAPH 1999*, Computer Graphics Proceedings, Annual Conference Series, pages 121–128. ACM, ACM Press / ACM SIGGRAPH.

Stam, J. and Fiume, E. (1995). Depicting fire and other gaseous phenomena using diffusion processes. In *Proceedings of SIGGRAPH 1995*, Computer Graphics Proceedings, Annual Conference Series, pages 129–136. ACM, ACM Press / ACM SIGGRAPH.

Sudo, S., Hashimoto, H., Ikeda, A., and Katagiri, K. (1987). Some studies of magnetic liquid sloshing. *Journal of Magnetism and Magnetic Materials*, 65(2):219–222.

Thomaszewski, B., Gumann, A., Pabst, S., and Strasser, W. (2008). Magnets in motion. In *Proceedings of SIGGRAPH Asia 2008*, Computer Graphics Proceedings, Annual Conference Series, pages 162:1–162:9. ACM, ACM Press / ACM SIGGRAPH Asia.

Yngve, G. D., O'Brien, J. F., and Hodgins, J. K. (2000). Animating explosions. In *Proceedings of SIGGRAPH 2000*, Computer Graphics Proceedings, Annual Conference Series, pages 29–36. ACM, ACM Press / ACM SIGGRAPH.

Yoshikawa, G., Hirata, K., Miyasaka, F., and Okaue, Y. (2011). Numerical analysis of transitional behavior of ferrofluid employing mps method and fem. *Magnetics, IEEE Transactions on*, 47(5):1370–1373.

Yu, J. and Turk, G. (2010). Reconstructing surfaces of particle-based fluids using anisotropic kernels. In *Proceedings of the 2010 ACM SIGGRAPH/Eurographics Symposium on Computer Animation*, pages 217–225. ACM, Eurographics Association.

APPENDIX A

Surface Deformation of Magnetic Fluid. In this appendix, we consider the case where the liquid surface is initially horizontal (the surface is equal to the *xy*-plane as shown in Fig. 12) (Cowley and Rosensweig, 1967). We apply a vertical magnetic field (in *z* direction) and calculate how the liquid surface changes according to the magnetic field. We show that we can obtain Equation (12) for describing the surface displacement according to the magnetic field. The variables of the density and magnetic field are defined as shown in Fig 12. When the liquid surface is slightly deformed (Fig. 13), the variation of the magnetic flux density inside the magnetic fluid, $\mathbf{b}_1 = \mathbf{B} - \mathbf{B}_0$, and the variation of the magnetic field, $\mathbf{h}_1 = \mathbf{H} - \mathbf{H}_{01}$ have the following relationship:

$$\mathbf{b}_1 = (\mu h_{1x}, \mu h_{1y}, \hat{\mu} h_{1z}), \tag{17}$$

where the magnetic flux density and the magnetic field are parallel. μ is the permeability, $\hat{\mu}$ is the differential permeability, h_{1x}, h_{1y}, h_{1z} show the *x*, *y* and *z* components of $\mathbf{h}_1$, since the magnetic flux density and the magnetic field are parallel. By letting the magnetic potential inside the magnetic fluid be ϕ_1 the magnetic field $\mathbf{h}_1$ in case of no electric current can be expressed as:

$$\mathbf{h}_1 = \nabla \phi_1. \tag{18}$$

If the electric current is flowing, the magnetic field due to electric currents must be considered and the potential term becomes complicate. By using the following equation,

$$\mathbf{H} = \nabla \cdot \mathbf{B}, \tag{19}$$

the divergence of the variation of the magnetic flux density can be rewritten as:

$$\nabla \cdot \mathbf{b}_1 = \mu \left(\frac{\partial^2 \phi_1}{\partial x^2} + \frac{\partial^2 \phi_1}{\partial y^2} \right) + \hat{\mu} \frac{\partial^2 \phi_1}{\partial z^2}. \tag{20}$$

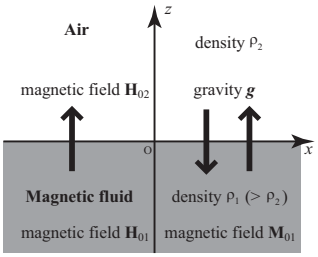

Figure 12: Horizontal interfacial boundary and vertical magnetic field. Each character equation of the fluid set as in the figure.

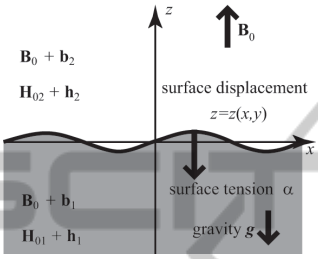

Figure 13: Deformation of the interfacial boundary by applied vertical magnetic field.

On the other hand, the magnetic field potential ϕ_2 above the magnetic fluid satisfies the following equation:

$$\left(\frac{\partial^2\phi_2}{\partial x^2}+\frac{\partial^2\phi_2}{\partial y^2}+\frac{\partial^2\phi_2}{\partial z^2}\right)=0. \tag{21}$$

Moreover, $\phi_1 = 0$ $(z \to -\infty)$ and $\phi_2 = 0$ $(z \to \infty)$ can be used as boundary conditions because each magnetic field is not affected by the deformation of the interfacial boundary at $z \pm \infty$. Due to the condition that the tangential component of magnetic field **H** is equal on both sides of the liquid surface, and the surface normal component of magnetic flux density **B** has the same value on both sides of the interface, the following equation is satisfied on the deformed liquid surface.

$$\begin{cases} \phi_1-\phi_2 = M_{01}z(x,y) \\ \hat{\mu}\frac{\partial\phi_1}{\partial z}-\mu_0\frac{\partial\phi_2}{\partial z}=0, \end{cases} \tag{22}$$

where, $M_{01} = |\mathbf{M}_{01}|$, $z(x, y)$ is the height field of the deformed liquid surface. Then, the following equations satisfy Equation (20), (21) and (22) and the boundary condition.

$$\phi_1 = \frac{M_{01}}{1+\gamma}z(x,y)\exp\left(k\sqrt{\frac{\hat{\mu}}{\mu}}z\right), \tag{23}$$

$$\phi_2 = \frac{\gamma M_{01}}{1+\gamma}z(x,y)\exp(-kz), \tag{24}$$

where, $\gamma = \sqrt{\frac{\hat{\mu}\mu}{\mu_0^2}}$ and $z(x, y)$ must satisfy the following equation:

$$\left(\frac{\partial^2}{\partial x^2}+\frac{\partial^2}{\partial y^2}+k^2\right)z(x,y)=0, \tag{25}$$

The general solution of this equation is the one shown in Equation (12).

APPENDIX B

Equilibrium of Force inside Spike Shape. In this appendix, we explain that the minimum value of the magnetization is represented as Equation (16) when the magnetic fluid forms a spike shape. Considering the balance between the surface tension and the difference in the stress on both sides of the liquid surface, the equilibrium equation of forces at the liquid surface can be represented by the following equation when the spike is formed.

$$(T_{zz}n_z)_1-(T_{zz}n_z)_2-\alpha\left(\frac{\partial^2}{\partial x^2}+\frac{\partial^2}{\partial y^2}\right)z=0, \tag{26}$$

where T_{zz} is the normal stress in z direction and n_z is the normal vector of z-axis. In the air and the magnetic fluid, T_{zz} can be written as follows, considering the magnetic pressure.

$$\begin{aligned}(T_{zz}n_z)_1 &= -p_1+\tfrac{1}{2}(B_0H_{01}+H_{01}b_{1z}+B_0h_{1z}) \\ (T_{zz}n_z)_2 &= -p_2+\tfrac{1}{2}(B_0H_{02}+H_{02}b_{2z}+B_0h_{2z}).\end{aligned} \tag{27}$$

Substituting the following equation of pressure distribution in Equation (26),

$$\begin{aligned}p_1 &= -\rho_1 gz+\tfrac{1}{2}(B_0h_{1z}-H_{01}b_{1z}) \\ p_2 &= -\rho_2 gz+\tfrac{1}{2}(B_0h_{2z}-H_{02}b_{2z}),\end{aligned} \tag{28}$$

the following equation can be derived considering Equation (22) and (25),

$$\left\{(\rho_1-\rho_2)g-\frac{\gamma}{1+\gamma}k\mu_0M_{01}^2+\alpha k^2\right\}z(x,y)=const. \tag{29}$$

Because z is not zero when the spike is deformed, Equation (29) holds only when the constant on the right side and the term in parentheses on the left side are zero.That is,

$$M_{01}^2=\frac{1+\gamma}{\mu_0\gamma}\left\{(\rho_1-\rho_2)\frac{g}{k}+\alpha k\right\}. \tag{30}$$

If the magnetization of magnetic fluid is less than Equation (30), the liquid surface does not change. When $k = \sqrt{\frac{(\rho_1-\rho_2)g}{\alpha}}$, the right hand side of equation is minimum. The minimum value is shown in Equation (16).